



TITLE:

Dispersion relations of director fluctuations along the direction perpendicular to the helical axis in cholesteric liquid crystals

AUTHOR(S):

Yoshioka, J.; Takanishi, Y.; Yamamoto, J.

CITATION:

Yoshioka, J. ...[et al]. Dispersion relations of director fluctuations along the direction perpendicular to the helical axis in cholesteric liquid crystals. EPL (Europhysics Letters) 2012, 98(1): 16006.

ISSUE DATE:

2012-04-01

URL:

<http://hdl.handle.net/2433/155560>

RIGHT:

© IOP Publishing 2012; This is not the published version. Please cite only the published version.; この論文は出版社版ではありません。引用の際には出版社版をご確認ご利用ください。

Dispersion relations of director fluctuations along the direction perpendicular to the helical axis in
cholesteric liquid crystals

J. Yoshioka, Y. Takanishi and J. Yamamoto

Department of Physics, Graduate School of Science, Kyoto University
Kita-Shirakawa, Kyoto 606-8502, Japan

PACs number: 61.30.-v, 42.70.Df, 78.35.+c

We theoretically analyzed dispersion relations of director fluctuations along the direction perpendicular to the helical axis in cholesteric liquid crystals, and experimentally verified validity of the analysis by dynamic light scattering (DLS) measurement. It is found that the dispersion relations are well-explained by two independent modes, which we call ‘splay-bend’ and ‘undulation’ modes.

1 After invention of the polymer stabilized blue phase in 2002, development of the next-generation
2 displays utilizing fast response of Kerr effect in the blue phase has been extensively performed [1-3].
3 However, its dynamic response against the electric field is not so sufficiently understood because of
4 complexity caused by the existence of the three-dimensional lattice composed of double twist
5 cylinders, in which cholesteric helical axes are locally extended radially in the plane normal to the
6 cylinder rod. In fact, the hydrodynamic modes of the orientation fluctuations are not described
7 completely even in the conventional cholesteric phase. Pseudo layer structure exists along the helix
8 in the cholesteric phase, and can be responded elastically against the uniaxial dilation or compression
9 of the helix. Thus, eigen modes for the distortion of director in the nematic phase are forbidden or
10 coupled with other modes as similar to the smectic phase. In order to understand the relation
11 between dynamics and response of the director in the blue phase, it is important to understand the
12 description of complete set of the hydrodynamic modes in the cholesteric phase first.

13 In the nematic phase, hydrodynamic modes of the orientation fluctuation have been completely
14 described by the individual three modes called splay, twist and bend modes [4]. On the other hand,
15 in the cholesteric phase, the hydrodynamic modes depend on whether wave vector is along parallel
16 or perpendicular to its helical axis. The mode parallel to the helical axis has already been analyzed
17 theoretically, and it has turned out that the dispersion relations are described by two modes, which
18 are called ‘twist’ and ‘viscous-splay’ (‘umbrella’) modes [4-6]. They have also been verified
19 experimentally, using dynamic light scattering (DLS) [7, 8]. Later, fluctuations of tensor
20 order-parameter modes parallel to the helical axis are also calculated [9]. In contrast, for the mode
21 perpendicular to the helical axis, there are few investigations, which have only been done for the case
22 in which the wave number of scattering vector q , which is defined as the difference between the wave
23 number vectors of the incident and the scattered light is much less than that of the helical pitch q_0 ,
24 which is defined by $q_0=2\pi/P$, where P is helical pitch length ($q \ll q_0$) [6, 10]. By the way,
25 order-parameter fluctuations in the isotropic phase above the cholesteric phase are also investigated

as the pretransitional behavior [11, 12].

In this paper, we focus on the hydrodynamic modes perpendicular to the helical axis in the cholesteric phase. Without assuming $q \ll q_0$, we analytically calculated the dispersion relations of the fluctuations in case that the scattering vector is perpendicular to the helical axis, and verified validity of the analysis experimentally using DLS.

From the macroscopic point of view, it can be considered that the cholesteric liquid crystal has pseudo-layer structure derived from its helix, and we assumed that it deforms without breaking and compressing the pseudo-layer structure. According to the layer deformation in the smectic A phase, small deformation of the pseudo-layer structure is written by the displacement u from the equilibrium configuration as shown in Fig. 1(b), and the increase of the elastic free energy is written using u as similar to the smectic phase. On the other hand, the elastic free energy density per unit volume of the cholesteric liquid crystal is usually written using the director \mathbf{n} [4]. Small deformation of the director from the equilibrium configuration $\delta\mathbf{n}$ has two components δn_ϕ and δn_z along perpendicular and parallel to the helical axis, where we assumed that z axis is parallel to the helical axis in the non-deformed state. Using them, we can write the director with small deformation as follows,

$$\mathbf{n} = (\cos q_0 z - \delta n_\phi \sin q_0 z, \sin q_0 z + \delta n_\phi \cos q_0 z, \delta n_z) . \quad (1)$$

Although δn_ϕ is independent of u , there is a relationship between δn_z and u ,

$$\delta n_z = \frac{\partial u(r, \phi)}{\partial r} \cos(\phi - q_0 z) , \quad (2)$$

where we adopted cylindrical coordinate system (r, ϕ, z) . Hence, we calculated total elastic free energy F derived from the small fluctuations, using δn_ϕ , and u instead of δn_z . We expand F in a Fourier series,

$$F = \frac{1}{2V} \sum_{\mathbf{k}} \left[\left(\frac{K_1 + K_3}{2} k_r^2 + K_2 k_z^2 \right) |\delta n_\phi(\mathbf{k})|^2 + \frac{3K_3}{8} k_r^4 |u(\mathbf{k})|^2 \right] , \quad (3)$$

where K_1 , K_2 and K_3 are elastic constants corresponding to splay, twist, and bend deformations of

1 local nematic director respectively, and V is volume of a sample. k_r and k_z are wavenumbers normal
2 and parallel to the helical axis, respectively.

3 Using the total free energy expressed in eq. (3), we calculated hydrodynamic equations for δn_ϕ and
4 u respectively. Here, we assume that the flow field is zero. From the balance of molecular field
5 and rotational viscosity, the hydrodynamic equation for δn_ϕ is written as

$$6 \quad -\left(\frac{K_1 + K_3}{2}k_r^2 + K_2k_z^2\right)\delta n_\phi(\mathbf{k}) = \gamma_1 \frac{d\delta n_\phi(\mathbf{k})}{dt}, \quad (4)$$

7 where γ_1 is a rotational viscosity. Time evolution of δn_ϕ indicates the exponential decay function,
8 and its relaxation frequency $1/\tau_\phi$ is written as

$$9 \quad \frac{1}{\tau_\phi} = \frac{(K_1 + K_3)}{2\gamma_1}k_r^2 + \frac{K_2}{\gamma_1}k_z^2. \quad (5)$$

10 We call this relaxation ‘splay-bend mode’, which shows splay and bend deformations of the
11 director in the plane perpendicular to the helical axis as shown in Fig. 1(a). From eq. (5), it is found
12 that this mode has both components parallel and perpendicular to the helical axis. This expression
13 is the same as the ‘phase mode’ which is one of the director fluctuation modes observed in the chiral
14 smectic C* phase with a helical structure[13,14].

15 On the other hand, from the analogy with lyotropic lamellar phase, the hydrodynamic equation for
16 u is written as [15]

$$17 \quad -\frac{3K_3}{8}k_r^2u(\mathbf{k}) = \eta \frac{du(\mathbf{k})}{dt}, \quad (6)$$

18 where η is a viscosity constant for the undulation deformation. Time evolution of u also indicates
19 the exponential decay function, and its relaxation frequency $1/\tau_u$ is written as

$$20 \quad \frac{1}{\tau_u} = \frac{3K_3}{8\eta}k_r^2. \quad (7)$$

21 We call this relaxation ‘undulation mode’, which shows the undulation deformation of the
22 pseudo-layer structure as shown in Fig. 1(b). Eq. (7) indicates that this mode has only the

1 component normal to the helical axis.

2 We measured experimentally the relaxation frequencies of the two modes in two scattering
3 geometries as shown in Figs. 2(a) and (b), which are suitable for measuring the splay-bend and
4 undulation modes, respectively. In Fig. 2(a), the helical axis is parallel to the incident light, while it
5 is perpendicular to scattering plane in Fig. 2(b). Here, we measured them with the scattering angle
6 θ being relatively small (18~45 degrees), so that the scattering vector \mathbf{q} is almost perpendicular to the
7 helical axis in both of the two geometries, and the director fluctuation modes having k_r are observed
8 in the two geometries. The scattering vector \mathbf{q} is defined by $\mathbf{q}=\mathbf{k}_i-\mathbf{k}_f$, where \mathbf{k}_i and \mathbf{k}_f are wave
9 number vectors of incident and scattered lights respectively, and wave number of scattering vector is
10 written as $q=|\mathbf{q}|=4\pi n/\lambda$ assuming quasi-elastic scattering, where n is the mean refractive index of
11 cholesteric liquid crystals and λ wave length of incident light. It is noted that both splay-bend and
12 undulation modes do not include the scattering geometry where the scattering vector is near parallel to the
13 helical axis, as a consequence of the incompressible condition of the layer of the helix.

14 The scattered field derived from director fluctuations is proportional to $\mathbf{f} \cdot (\boldsymbol{\varepsilon}(\mathbf{q}, t) \mathbf{i})$, where $\boldsymbol{\varepsilon}(\mathbf{q}, t)$
15 is the Fourier transformation of the relative dielectric tensor $\boldsymbol{\varepsilon}(\mathbf{r}, t)$, and \mathbf{i} and \mathbf{f} are polarizations of
16 incident and scattered lights respectively [4]. The $\boldsymbol{\varepsilon}(\mathbf{r}, t)$ of the cholesteric liquid crystals is
17 written as $\varepsilon_{\alpha\beta} = \varepsilon_{\perp} \delta_{\alpha\beta} + \varepsilon_a n_{\alpha} n_{\beta}$, where ε_{\perp} is the dielectric constant for the ordinary light, and ε_a
18 is the dielectric anisotropy. Furthermore, we assumed that the polarizations of the incident and the
19 scattered light are not modulated even in the cholesteric samples. Although this assumption is quite
20 different from real system, it is much more difficult and complex to consider the polarization of
21 incident and scattered light strictly in the cholesteric liquid crystals. In the previous studies as
22 shown in references [5, 7, 8], the autocorrelation functions were theoretically analyzed without
23 discussing the modulations of the polarizations in the cholesteric samples, and experimental results
24 were well-explained using the analysis, so that we adopted the above assumption. Using them, we
25 calculated time autocorrelation functions of scattering intensity, which is proportional to
26 $\langle \mathbf{f} \cdot (\boldsymbol{\varepsilon}(\mathbf{q}, 0) \mathbf{i}) \mathbf{f} \cdot (\boldsymbol{\varepsilon}^*(\mathbf{q}, t) \mathbf{i}) \rangle^2$ in the two scattering geometries. As a result, it is found that the
27 undulation modes are observed with wave numbers $\mathbf{k} = \mathbf{q} + \mathbf{q}_0$ and $\mathbf{q} - \mathbf{q}_0$ in Figs. 2(a) and (b), while
28 the splay-bend mode is only observed with wave numbers $\mathbf{k} = \mathbf{q} + 2\mathbf{q}_0$ and $\mathbf{q} - 2\mathbf{q}_0$ in Fig. 2(a), where

\mathbf{q}_0 is defined by $\mathbf{q}_0=(0, 0, q_0)$. Hence we call Fig. 2(a) ‘splay-bend geometry’ and Fig. 2(b) ‘undulation geometry’. Substituting these conditions into eqs. (5) and (7), the relaxation frequencies of the two modes are given by

$$\frac{1}{\tau_\phi} = \frac{(K_1 + K_3)}{2\gamma_1} q^2 + \frac{4K_2 q_0^2}{\gamma_1}, \quad (8a)$$

$$\frac{1}{\tau_u} = \frac{3K_3}{8\eta} q^2. \quad (8b)$$

The experiment was performed in the cholesteric phase of the mixture of 7CB, MLC6427 and MLC6248, which is optical isomer of MLC6247 (Merck). We fixed weight ratio of the 7CB and the chiral dopant mixture of MLC6247 and MLC6248 to be 7:3. Furthermore, adjusting weight ratio of MLC6247 and MLC6248, we prepared the samples whose physical pitch lengths are between 300 and 820nm. Not depending on the mixing ratio, the mixtures showed almost the same phase sequence, which is isotropic–42C–cholesteric. In this experiment, we fixed the temperature at 30C.

For the DLS measurement, we prepared 10μm thick sandwich cells made of two glass substrates. Since the incident light is almost perpendicular to the substrates in our measurement system, we need to align the helical axis perpendicular to the substrates for the splay-bend geometry (Fig. 2(a)), parallel to them for the undulation geometry (Fig. 2(b)). Hence, for the splay-bend geometry, we used commercial homogeneous planar cells, while for the undulation geometry, we adopted the method as shown in reference [16] to achieve the alignments in which the helical axis is parallel to the substrates.

Figure 3 shows the normalized autocorrelation functions of scattering intensity $g_2(t) - 1$ actually observed in the splay-bend (symbol ○) and undulation (symbol □) geometries respectively. In the splay-bend geometry, two relaxations are observed around ~0.04ms and ~0.8ms, while in the undulation geometry, single relaxation is observed around ~0.8ms, which is close to the slower mode observed in the splay-bend geometry. Hence, it is confirmed that the faster mode in the splay-bend geometry corresponds to the splay-bend mode, and the slower mode in the splay-bend and the single

1 mode in the undulation geometry correspond to the undulation mode, as described in the above
2 section.

3 Figure 4(a) shows the dispersion relations of the relaxation frequencies of the splay-bend mode
4 with respect to the wave numbers. The relaxation frequencies are proportional to the square of the
5 wave numbers, and its slope is independent of the helical pitch, while they show finite values
6 depending on the pitch in the limit $q \rightarrow 0$, which are proportional to the square of the wave numbers
7 of helical pitches as shown in Fig. 5. These behaviors are well-explained by eq. (8a). Figure 4(b)
8 shows the dispersion relations of the undulation mode measured in the undulation geometry. The
9 relaxation frequencies are proportional to the square of the wave numbers, and they become zero in
10 the limit $q \rightarrow 0$, not depending on the helical pitches. These behaviors are also well-explained by eq.
11 (8b).

12 To summarize, we theoretically analyzed dispersion relations of director fluctuations along the
13 direction perpendicular to the helical axis in the cholesteric liquid crystal without assumption of
14 $q \ll q_0$, and verified validity of the analysis using DLS measurement. In the analysis, assuming
15 that the cholesteric liquid crystals fluctuate without breaking its incompressible pseudo-layer
16 structures, we designed the ‘splay-bend’ and the ‘undulation’ modes as the director fluctuation modes,
17 which are expressed by eq. (8a) and (8b). Furthermore, it is found that the experimental results well
18 satisfies with our proposed dispersion relation of the two modes, and the assumption mentioned
19 above is also adequate.

20

21

22 Acknowledgement

23 We acknowledge Merck Ltd., Japan for supplying chiral dopants, MLC6247 and MLC6248. This
24 work was supported by the Grant-in-Aid for Scientific Research (B) (No.21740312), the JSPS

Core-to-Core Program “International research network for non-equilibrium dynamics of soft matter” and the Global COE Program "The Next Generation of Physics, Spun from Universality and Emergence" from the Ministry of Education, Culture, Sports, Science and Technology (MEXT) of Japan.

References

- [1] KIKUCHI H., YOKOTA M., HISAKADO Y., YANG H. and KAJIYAMA T., *Nature Materials*, **1** (2002) 64.
- [2] GE Z., GAUZA S., JIANO M., XIANYU H. and WU ST., *Appl. Phys. Lett.*, **94** (2009) 101104
- [3] RAO L., YAN J., WU ST., YAMAMOTO S. and HASEBA Y., *Appl. Phys. Lett.*, **98** (2011) 081109
- [4] DE GENNES P. G. and PROST J., *The Physics of Liquid Crystals second edition*, (Clarendon

- 1 Press Oxford) 1993.
- 2 [5] FAN C., KRAMER L. and STEPHEN M. J., *Phys. Rev. A*, **2** (1970) 2482.
- 3 [6] LUBENSKY T. C., *Phys. Rev. A*, **6** (1972) 452.
- 4 [7] BORSALI R., SCHROEDER U. P., YOON D. Y. and PECORA R., *Phys. Rev. E*, **58** (1998)
- 5 R2717.
- 6 [8] GIRIDHAR M. S. and SURESH K. A., *Eur. Phys. J. E*, **7** (2002) 167.
- 7 [9] PANTEA M. A. and KEYES P. H., *Phys. Rev. E*, **71** (2005) 031707.
- 8 [10] ADORJAN A., STOJADINOVIC S., SUKHOMLINOVIA L., TWEIG R. and SPRUNT S.,
- 9 *Phys. Rev. Lett.*, **90** (2003) 035503.
- 10 [11] YANG C. C., *Phys. Rev. Lett.* **28** (1972) 955.
- 11 [12] HARADA T., and CROOKER P. P., *Phys. Rev. Lett.*, **34** (1975) 20.
- 12 [13] DREVENSEK I., MUSEVIC I. and COPIC M., *Phys. Rev. A*, **41** (1990) 923.
- 13 [14] SUN H., ORIHARA H. and ISHIBASHI Y., *J. Phys. Soc. Jpn.*, **60** (1991) 4175.
- 14 [15] NALLET F., ROUX D. and PROST J., *J. Phys. France*, **50** (1989) 3147.
- 15 [16] HUNG W. -C., CHENG W. -H., LIN Y. -S., JANG D. -J., JIANG I. -M. and TSAI M. -S., *J.*
- 16 *Appl. Phys.*, **104** (2008) 063196.
- 17
- 18
- 19
- 20

1
2
3
4
5
6
7
8
9
10
11
12
13
14
15
16
17
18
19

Figure caption

Figure 1: (a) Director deformation in the splay-bend mode. Left-side figure shows three dimensional image of director configuration. Ellipsoids of right-side figure exhibit the director configuration at certain planes perpendicular to helical axis, and splay (top and bottom planes) and bend (middle plane) deformation are observed. (b) Director deformation in the undulation mode. Ellipsoids show director configuration, and solid lines indicate the deformation of pseudo-layer

1 structures from the equilibrium configuration shown in broken lines.

2

3 Figure 2: (a) Splay-bend and (b) undulation mode scattering geometries. \mathbf{q} is the scattering vector
4 and \mathbf{q}_0 is the wave number vector of the cholesteric helical pitch.

5

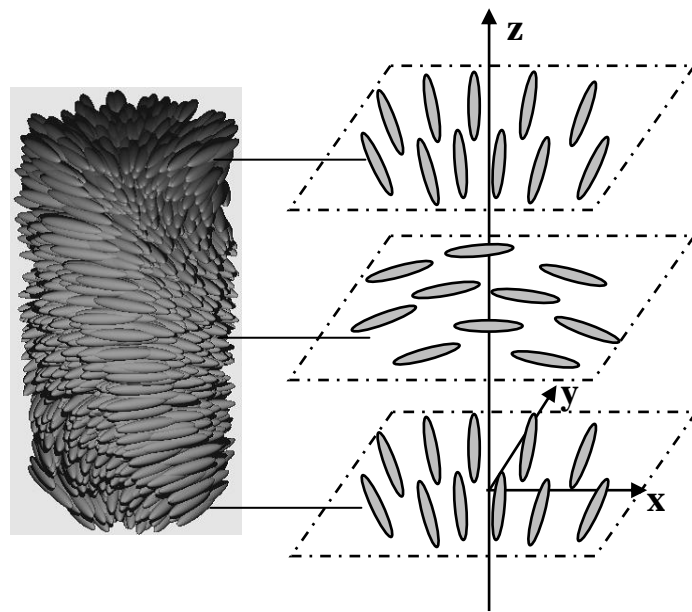
6 Figure 3: Autocorrelation functions measured in the two scattering geometries. Open circle and
7 square show the data measured in the splay-bend and undulation geometries respectively, and well
8 fitted by double and single exponential curves respectively. The scattering angle is 24° , the
9 temperature 30°C , and the physical pitch length of the sample 430nm .

10

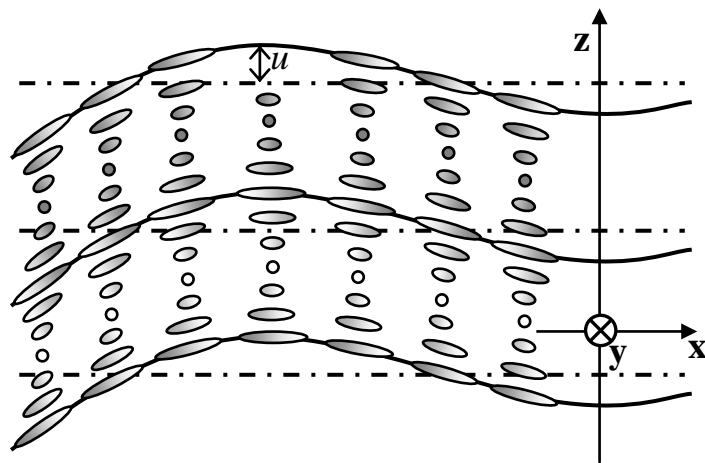
11 Figure 4: Dispersion relations of the two modes, (a) splay-bend and (b) undulation modes in various
12 mixtures. Fitted straight lines calculated by eq. (8a) and (8b) respectively are also shown, and it is
13 found that the slope of the fitted lines is independent of the helical pitch. Fitting parameters are $(K_1$
14 $+ K_3) / 2\gamma_1 = (1.1 \pm 0.2) \times 10^{-10} \text{ m}^2/\text{s}$ and $3K_3 / 8\eta = (1.8 \pm 0.2) \times 10^{-11} \text{ m}^2/\text{s}$.

15

16 Figure 5: Extrapolation values of relaxation frequency of the splay-bend mode in the limit $q \rightarrow 0$ as a
17 function of square of wave number of the helical pitch. Broken line is fitted using eq. (8a), in
18 which $4K_2 / \gamma_1$ is $7.2 \times 10^{-11} \text{ m}^2/\text{s}$.



(a)



(b)

Fig.1

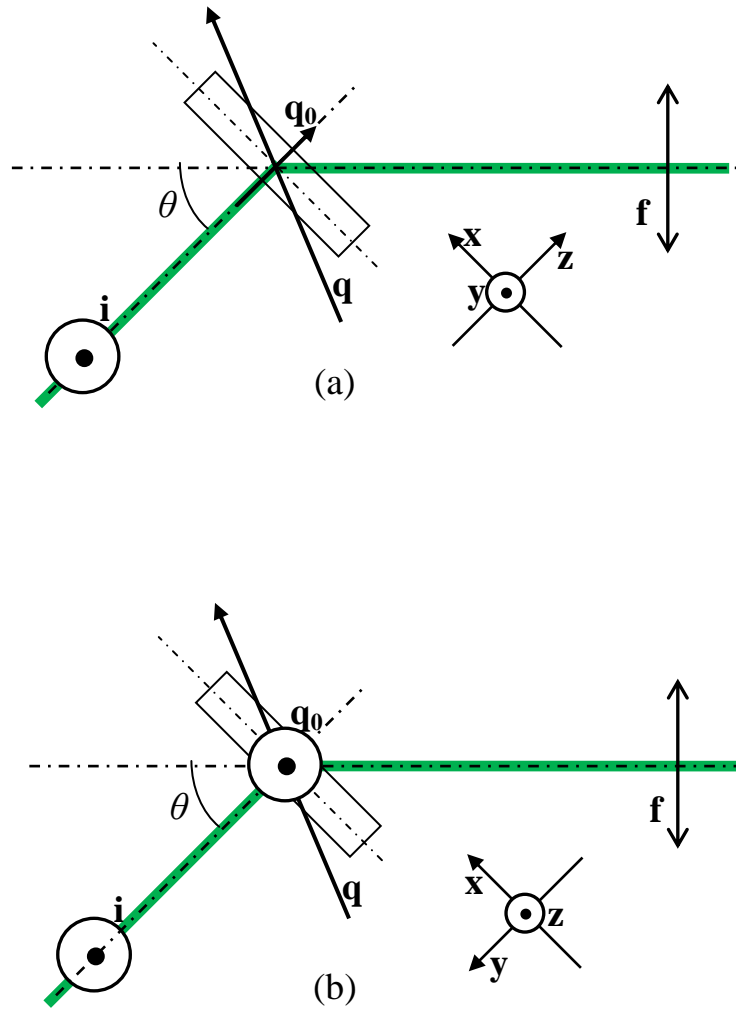


Fig. 2

Figure 3

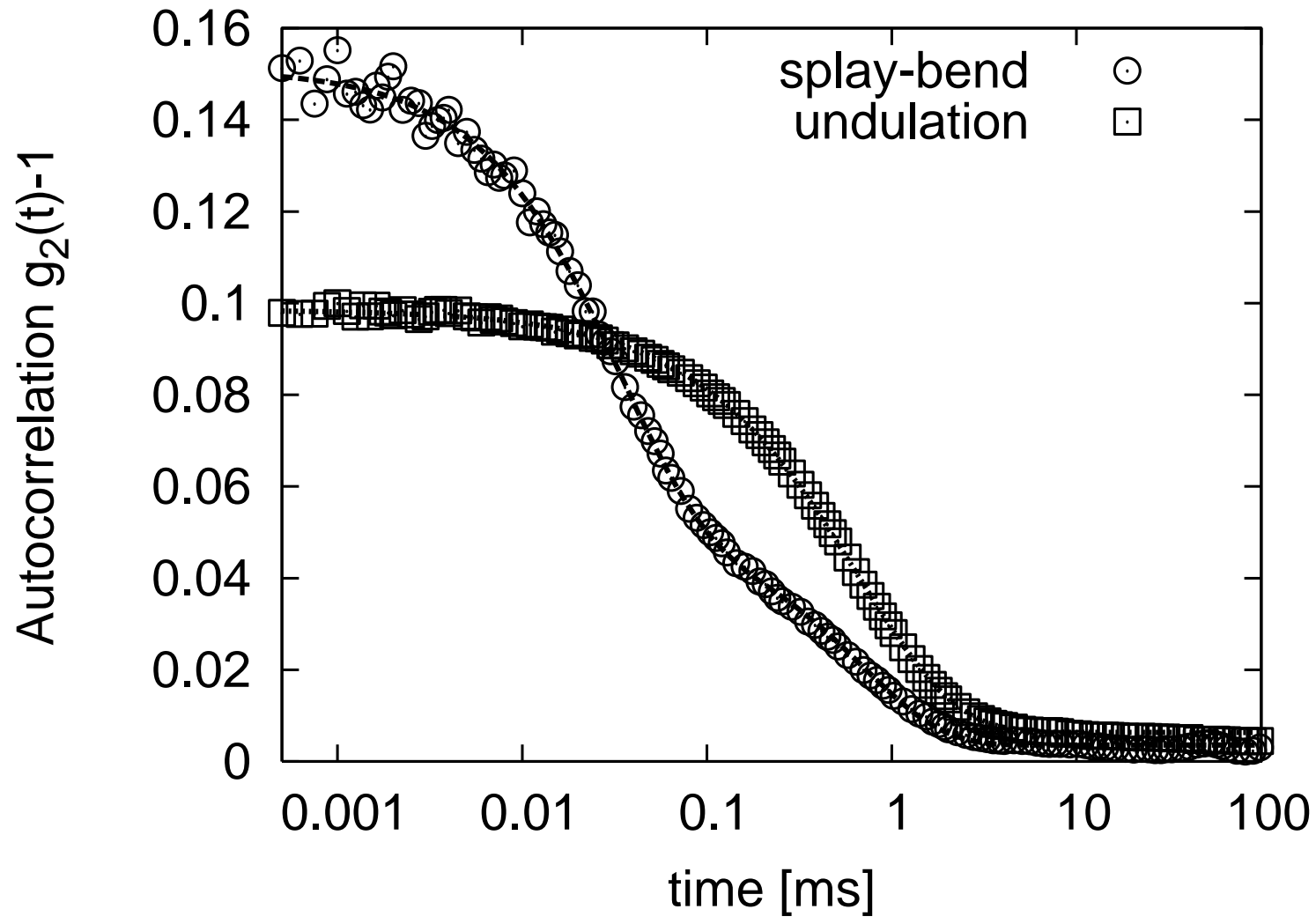


Figure 4(a)

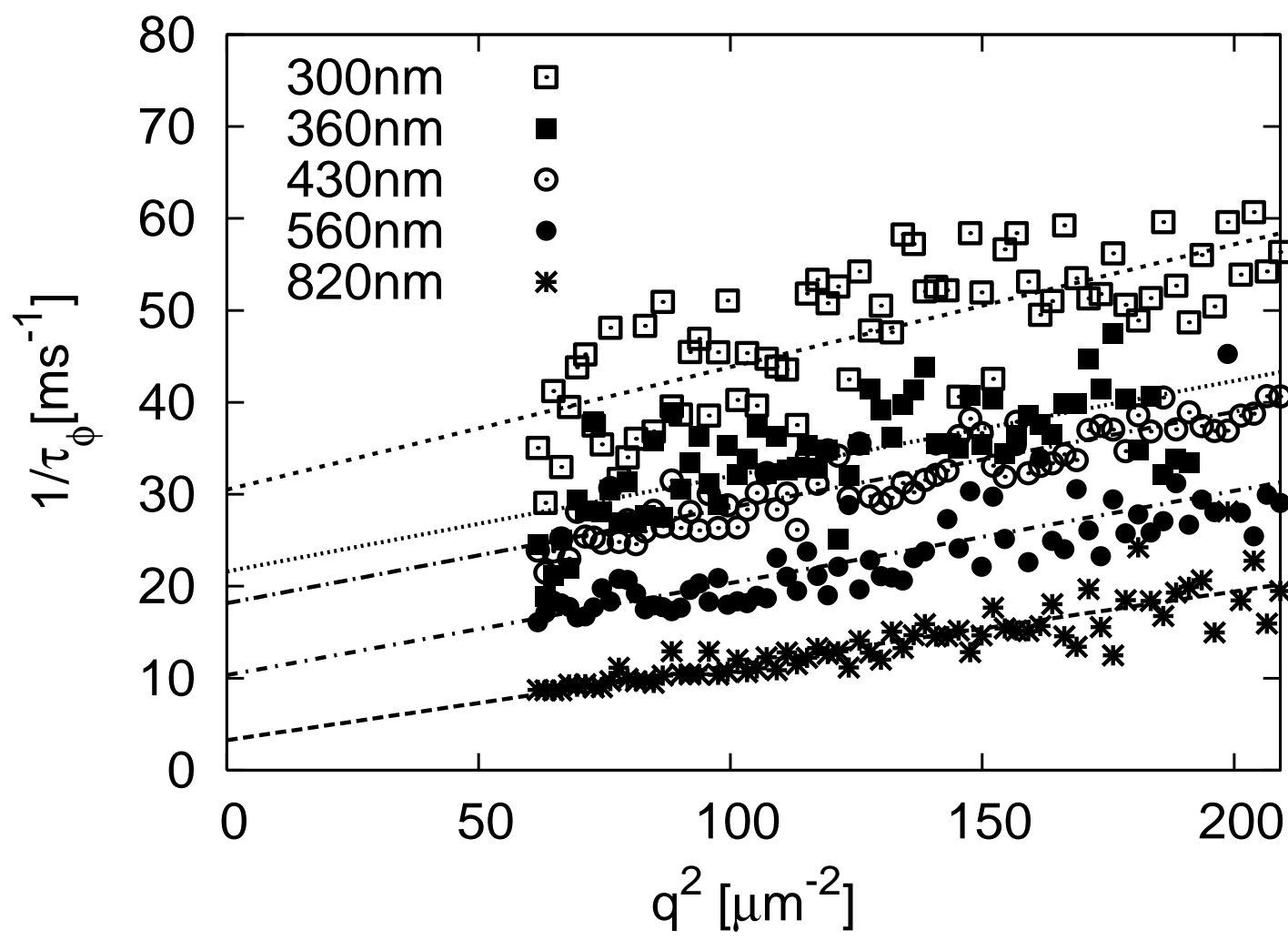


Figure 4(b)

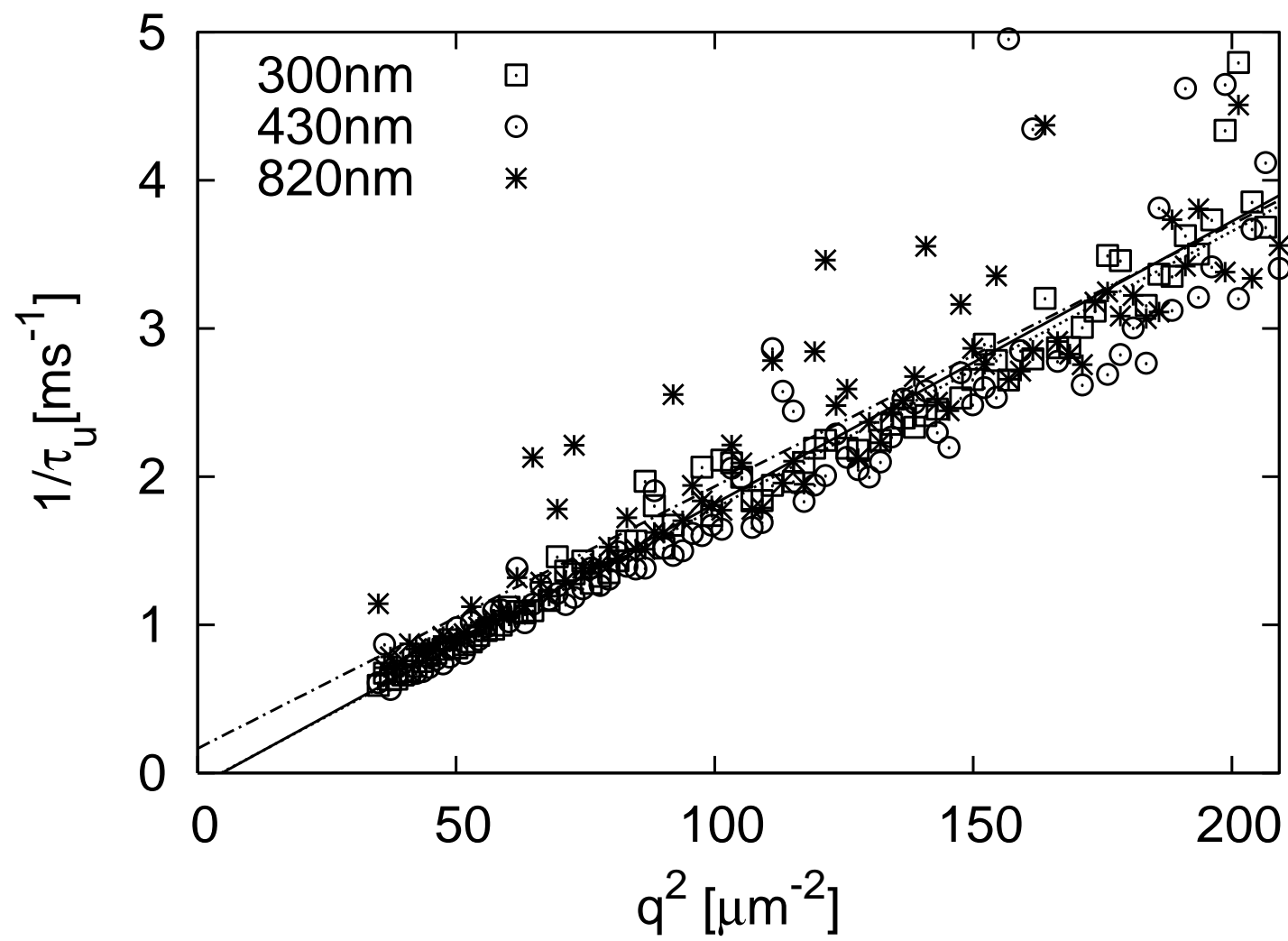


Figure 5

